145, 237.
13. Leherte, L.; Andre, J. M.; Vercauteren, D. P.; Derouane, E. G. *J. Molec. Catal.* **1989**, *54*, 426.
14. Leherte, L.; Andre, J. M.; Derouane, E. G.; Vercauteren, D. P. *Comput. Chem.* **1991**, *15*, 273.
15. Leherte, L.; Andre, J. M.; Derouane, E. G.; Vercauteren, D. P. *J. Chem. Soc., Faraday Trans.* **1991**, *87*, 1959.
16. Pickett, S. D.; Nowak, A. K.; Thomas, J. M.; Peterson, B. K.; Swift, J. F. P.; Cheetham, A. K.; den Ouden C. J. J.; Smit, B.; Post, M. F. M. *J. Phys. Chem.* **1990**, *94*, 1233.
17. Nowak, A. K.; den Ouden C. J. J.; Pickett, S. D.; Smith, B.; Cheetham, A. K.; Post, M. F. M.; Thomas, J. M. *J. Phys. Chem.* **1991**, *95*, 848.
18. Shin, J. M.; No, K. T.; Jhon, M. S. *J. Phys. Chem.* **1988**, *92*, 4533.
19. Moon, G. K.; Choi, S. G.; Kim, H. S.; Lee, S. H. *Bull. Kor. Chem. Soc.* **1992**, *13*, 317.
20. Moon, G. K.; Choi, S. G.; Kim, H. S.; Lee, S. H. *Bull. Kor. Chem. Soc.* **1993**, *14*, 356.
21. Lee, S. H.; Moon, G. K.; Choi, S. G.; Kim, H. S. *J. Phys. Chem.* **1994**, *98*, 1561.
22. Choi, S. G.; Lee, S. H. *Mol. Sim.* **1996**, *17*, 113. In Figs. 2, 3, 4, and 5, NH4(2) and NH4(3) should be replaced by each other.
23. Lee, S. H.; Choi S. G. *J. Phys. Chem.* B **1997**, *101*, 8402.
24. Pluth, J. J.; Smith, J. V. *J. Am. Chem. Soc.* **1980**, *102*, 4704.
25. Pluth, J. J.; Smith, J. V. *J. Am. Chem. Soc.* **1983**, *105*, 1192.
26. Jang, S. B.; Han, Y. W.; Kim, D. S.; Kim, Y. *Kor. J. Crystal.* **1990**, *1*, 76.
27. Seff, K.; Shoemaker, D. P. *Acta Crystallogr.* **1967**, *22*, 162
28. Gramlich, V.; Meier, W. M. *Z. Kristallogr.* **1971**, *133*, 134.
29. McCusker, L. B.; Seff, K. *J. Am. Chem. Soc.* **1981**, *103*, 3441.
30. Nicholas, J. B.; Hopfinger, A. J.; Trouw, F. R.; Iton, L. X. *J. Am. Chem. Soc.* **1991**, *113*, 4792
31. Faux, D. A.; Smith, W.; Forester, T. R. *J. Phys. Chem.* B **1997**, *101*, 1762.
32. Yanagida, R. Y.; Amaro, A. A.; Seff, K. *J. Phys. Chem.* **1973**, *77*, 805.
33. (a) de Leeuw, S. W.; Perram, J. W.; Smith, E. R. *Proc. R. Soc. London* **1980**, *A373*, 27. (b) Anastasiou, N.; Fincham, D. *Comput. Phys. Commun.* **1982**, *25*, 159.
34. Genechten, K. A. V.; Mortier, W. J. *Zeolites* **1988**, *8*, 273.
35. Gauss, K. F. *J. Reine. Angew. Math.* **1829**, *IV*, 232.
36. Gear, C. W. *Numerical initial value problems in ordinary differential equation*; Englewood Cliffs NJ; Prentice-Hall, 1971.
37. Willis, B. T. M.; Pryor, A. W. *Thermal vibrations in Crystallography*; Cambridge University Press; Cambridge, 1975.
38. Johnson, C. K. ORTEP: A FORTRAN *Thermal Ellipsoid Plot Program*; ORNL-3794, Oak Ridge National Laboratory, Oak Ridge, TN, 9165.
39. Lee, S. H.; Choi, S. G. in preparation.
40. Behrens, P. H.; Wilson, K. R. *J. Chem. Phys.* **1981**, *74*, 4872.

Thermal Decomposition of PVB (polyvinyl butyral) Binder in the MCFC (molten carbonate fuel cell)

Jung Ju Seo*, Ji Young Kim†, and Keon Kim†

Korea Basic Science Institute Seoul Branch, 126-16 Anam-dong, Sungbuk-Ku, Seoul 136-701, Korea
†Department of Chemistry, Korea University, 1 Anam-dong, Sungbuk-Ku, Seoul 136-701, Korea
Received November 1, 1997

The thermal decomposition of matrix-green sheet and electrolyte-green sheet in CO_2, sintering effect of Ni-green sheet for the decomposition of matrix-green sheet, and binder burnout during MCFC unit cell operation were studied. Binders decomposed incompletely in CO_2 and thermal decomposition of electrolyte-green sheet was affected more than that of matrix-green sheet by CO_2. It was important to decompose the binder completely before it changed to nonoxidative condition. Binders were more effectively eliminated in the sintered Ni-matrix green sheet than Ni-matrix green sheet. The decomposition state of binder during unit cell operation was showed by analyzing the produced gases. Two characteristic peaks, butanal and butene were detected at all experimental condition and binder burnout state was checked by analyzing the change of two index peaks during decomposition process. Most of binders in the unit cell were decomposed sufficiently under slow heating rate and initial oxidative condition.

Introduction

A fuel cell is a device that directly converts the chemical energy of reactants into electric energy by electrochemical reactions. Molten carbonate fuel cells (MCFCs) are presently under development for electric utility power generation.

MCFCs have high efficiency which is due to their low polarization, the possibility of internal reforming, and the their high-grade waste heat.[1]

MCFC is composed of electrodes, a molten carbonate electrolyte and a matrix. A typical fabrication process for major components involves tape-casting an appropriate mixture of metallic substrate, binders, and various additives. In combination with appropriate plasticizer, binder is used to modify the rheological properties of the casting and to provide strength and flexibility needed for handling and green machining operations.[2] Polymeric binder is most frequently removed by thermal decomposition. Incomplete burnout can adversely affect subsequent densification behavior, as well as degrade the physical properties of the ceramic. Burning out clearly with minimum of warpage to the fired part is one of the important factors of binder.[3]

PVB (polyvinyl butyral) is widely used as a binder in ceramic processing and it is prepared from aldehyde and polyvinyl alcohols. The typical fraction of PVB is: $B \leq 20\%$ and $C \leq 2\%$ (See the next formula).

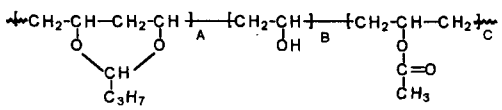

Both free radical reaction and intramolecular elimination reaction produce the main decomposition product, butanal, and the water arises from dehydration of vinyl alcohol unit[4]:

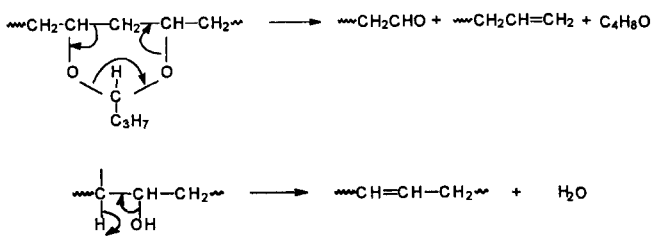

In the tape casting process or ceramic fabrication process, it is important to control the burnout of the organic additives both to prevent crack and to minimize a residual carbon that may inhibit sintering. All organic additives must be removed during firings before sintering begins and maintain a proper condition to the ceramics such as porous structure. The effort to find optimal removal conditions is ongoing.[5-8] It is known that various metal substrates can interact with polymer binders during binder burnout and this interaction affect polymer thermal degradation process. The thermal degradation of PVB polymer is enhanced by presence of metal substrates but leave carbon residue that is presumably bonded to metal oxide surface. The thermal decomposition and the elimination of binder are important factors to operate the fuel cell smoothly.[9]

Water vapor is often added to nonoxidative sintering atmospheres to remove carbon that forms during binder burnout. The wet atmosphere may be either oxidizing or reducing to the refractory metal component of substrate. Simultaneously, the carbonaceous residue reacts with water vapor to form carbon monoxide and hydrogen gas.[10]

CO_2 is an indispensable gas to operate MCFC. Therefore, it is necessary to investigate the influence of CO_2 for the thermal decomposition of PVB binders. Compared to the thermal decomposition of PVB binder in air, PVB may decompose somewhat differently in the MCFC operation. This is expected because air makes enough oxidative condition to decompose binders but CO_2 does not.

In the MCFC operation, polymer binders should decompose completely during the early stage of heating. Although complete polymer decomposition can usually be achieved in oxidative atmospheres, incomplete binder burnout can often occur in the inert or reductive atmospheres that are required for operating fuel cell. Moreover, there is no method to detect the burnout state of binders during fuel cell operation. To find the proper decomposition condition of PVB binder in MCFC, we have been studied the thermal decomposition of pure PVB and green sheets of each component in MCFC. We found that butanal and butene peaks among the decomposition products showed a characteristic decomposition behavior.[11] Thus, these two peaks can be used as an index to detect the extent of binder decomposition during the unit cell operation.

In the present paper, we report the decomposition of binder in the green sheet pair in oxidative condition and thermal decomposition of matrix-green sheet and electrolyte-green sheet in CO_2. Finally in the investigation of the decomposition behavior of binder during the unit cell operation, we tried to apply previous results to check the burnout state of binder in the real unit cell system and optimize the binder burnout conditions in the MCFC.

Experimental

Materials. The PVB used in this study was Butvar B-98 (Monsanto). Green sheets were made by the tape-casting method. An electrolyte-green sheet was 3.5 g of Li_2CO_3/K_2CO_3 (62/38 m/o) with 14 wt.% PVB and the matrix-green sheet was 2.5 g of γ-$LiAlO_2$ with 20 wt.% PVB. Each amount of samples were reduced by half for green sheet pair experiment. The Ni-green sheet was 2.5 g of Ni (INCO #255) with 20 wt% PVB and sintering at 850 °C for 30 min in 20% H_2/ 80% N_2 for making sintered Ni sheet. Green sheets were dried at 100 °C for 15hr to evaporate residual solvent and additives, then transferred to a desiccator.

Instrumentation. To make air-containing water vapor, a supporting apparatus was produced.[12] The feed gas was generated by bubbling air through de-ionized water kept at 50 °C and this apparatus was connected to the furnace. The decomposed gases through the furnace were collected by a gas-tight syringe at the hot stage and immediately analyzed by GC and GC/MS at every 100 °C. The total gas flow-rate was 100mL/min and the heating rate of furnace was 2 °C/min.

Gas chromatographic analysis was carried out with a HP 5890 (Hewlett-Packard) Gas Chromatography equipped with a flame ionized detector, a 12 m × 0.32 mm Polaplot-Q (CHROMPACK Co.) column with a 20 μm film thickness and a HP 3396A integrator. The sample was injected to GC with split-less. Temperature of the injection port and detector were 200 °C and 230 °C, respectively. The oven temperature was programmed with a initial hold for 2 min at 30 °C, followed by an increase at 10 °C/min to 230 °C, with a hold for 10 min. Nitrogen carrier gas flow was 1 mL/min and nitrogen make-up gas was set at 30 mL/min.

Table 1. The dimension of each part in the unit cell

Part	Dimension (W×L×H)
anode	5 cm×6 cm×0.05 cm
cathode	5 cm×6 cm×0.05 cm
matrix×2	7 cm×7 cm×0.05 cm
electrolyte×3	7.5 cm×7.5 cm×0.06 cm
separator (Ag)	5 cm×6 cm×0.01 cm

Mass spectra were acquired by a HP5988 (Hewlett-Packard) mass spectrometer (MS) interfaced to a HP 5890GC unit scanning from m/z 10 to 250 at the rate of 30 spectra/min. Mass spectral library searches employed a 130, 544 spectra Wiley mass spectral library. All column conditions were the same as the GC conditions except for carrier gas. The mass-operating conditions were as follows; source temperature: 200 °C, electron energy: 70 eV, He carrier gas flow: 0.9 mL/min.

All of the relative comparison were made with the GC result and normalized for the total area. The GC/MS data were used only for the identification of peaks shown on GC chromatogram.

Unit cell. Each dimension of individual parts is on Table 1, and the unit cell was pressed by 2 kg/cm^2 to give a good contact.

The binder in unit cell was decomposed in air and oxygen until 470 °C. The unit cell was operated up to 650 °C, using a fuel gas (68% H_2/18% CO_2/14% H_2O) and a cathode gas (80% O_2/20% CO_2). The heating rate of each steps was 0.2 °C/min-0.4 °C/min. To prevent the loss of decomposed gases, we wrapped sides of the unit cell by the matrix seal containing all the component of the matrix-green sheet and collected gases produced in a gap between two electrodes until 470 °C. The decomposed gases were separately acquired in each gas outlet of electrodes after 470 °C (Figure 1).

Results and discussion

Thermal decomposition of electrolyte and matrix-green sheet in CO_2.

Off line furnace-GC and GC/MS were employed to generate and analyze the thermal degradation products formed from heated matrix-green sheet and electrolyte-green sheet samples to 700 °C in CO_2. Because CO_2 itself is the degradation product of PVB, CO_2 can not make an adequate oxidative condition. Consequently, supply of CO_2 gives an adverse effect to the decomposition process. In addition, the electrolyte-green sheet gets a supply of carbonate from CO_2 before decomposing binders completely in the green sheet.

Figure 2 indicates the total area changes of thermally decomposed gases, which were analyzed by GC in CO_2. The major peaks such as acetal, butanal, butenal, and butanol evolved from the matrix-green sheet were detected at 200 °C. Above 300 °C, the intensity of those major peaks were decreased but minor peaks such as aromatic carbon showed peak maxima around 300 °C. The total amounts of degradation products evolved from matrix-green sheet decreased continuously until 500 °C, then increased due to the contribution of butene peak above 600 °C. Thermal decomposition of binder was continued even at 700 °C. This means that binders in the matrix-green sheet did not decompose completely around the temperature corresponding to the peak maxima in CO_2.

The thermal decomposition of binder in the electrolyte-green sheet in CO_2 was more complicate than that of other green sheets. The electrolyte-green sheet itself contained carbonates and gas atmosphere was not sufficient to decompose the binder. The total amounts of degradation products evolved from electrolyte-green sheet decreased above 300 °C, but decomposition products were detected with a considerable amount even at higher temperature because CO_2 was provided continuously above the electrolyte melting temperature. Below 400 °C, the decomposition of binder in other conditions were completed over 80%, but decomposition of binder in the electrolyte-green sheet was completed less than 61% in CO_2. The decomposition of binder in the electrolyte-green sheet was affected by CO_2 more than that of matrix-green sheet. In the case of thermal decomposition in CO_2, the binders in the electrolyte-green sheet were decomposed incompletely compared with that of matrix-green sheet.

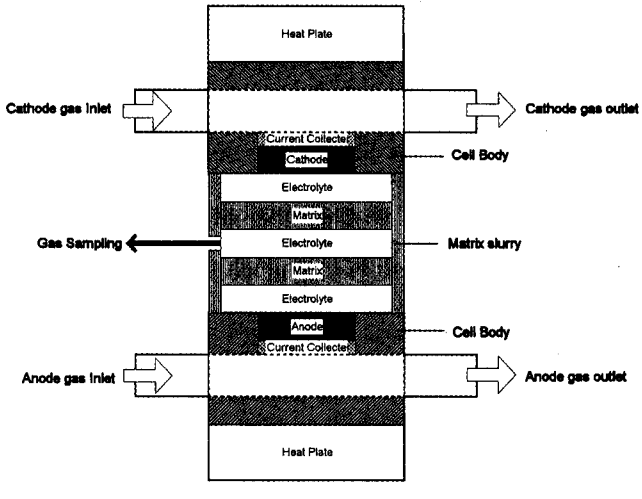

Figure 1. Schematic diagram of gas sampling position.

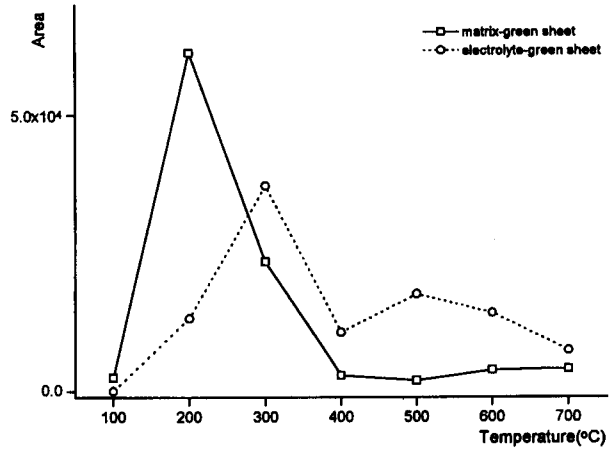

Figure 2. Total area *vs.* temperature plot of GC graphs in CO_2.

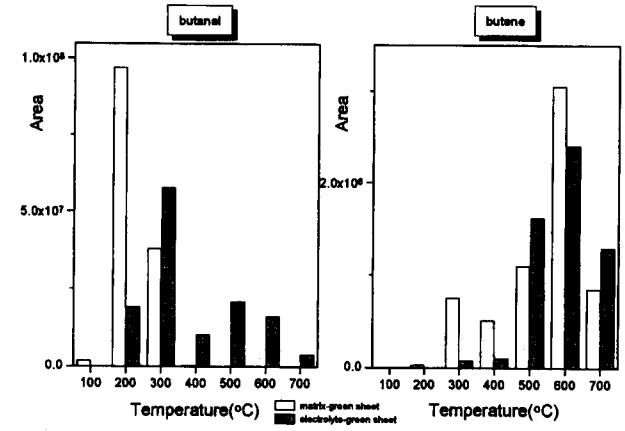

Figure 3. Relative area changes of matrix-green sheet and Ni-green sheet about temperature in CO_2.

Figure 3 shows temperature profiles of the index peaks that are obtained by GC analysis of the produced gases of the heated matrix-green sheet and electrolyte-green sheet. A main decomposition product, butanal shows a similar tendency to that of total area profile. The decomposition of binder in the matrix-green sheet shows a similar behavior to that in air, whereas the decomposition of binder in the electrolyte-green sheet is continued even at higher temperature. This means that even the side chain elimination did not occur sufficiently in CO_2.

The butene peak profile of Figure 3 indicates the termination state of decomposition process. Butene was detected even above 500 °C, because oxidative gases were not supplied enough to decompose binder polymers completely. Therefore, every binder must be burnout before CO_2 was mixed into the gases.

Thermal decomposition of electrolyte and matrix-green sheet in the mixed gas condition. To understand the thermal decomposition of binders in the MCFC, the decomposition of the binder in mixed gas condition as well as pure air and pure CO_2 must be checked. Figure 4 is the decomposition profile of binders in the matrix-green sheet and electrolyte-green sheet when the gases were changed from air (150 mL/min) to air (100 mL/min)/CO_2(50 mL/min) mixture gas at 320 °C followed by a 120 min isothermal period to decompose the PVB binder sufficiently. The binders in the both of green sheets were decomposed within the range of temperature narrower in mixed gas that in pure CO_2.

The amounts of produced butanal were decreased, but the intensity of other peaks such as butene, butenal, and butanol was getting stronger after in the mixture of CO_2 and air. Since polyvinyl butyral moieties comprised more than 80% of the polymer used in this study, butanal was responsible for most of the PVB decomposition. The amounts of produced gases from heated electrolyte-green sheet were slightly increased after the CO_2 gas was mixed with air. As the amounts of produced butene gases were increased with temperature, decreased total area of the GC chromatogram was increased above 400 °C as shown in Figure 4.

The total amounts of produced gases from the matrix-green sheet were not increased after the CO_2 gas was mixed, even though the amounts of butene were increased with temperature. This was because of late-elution of other minor gases produced from the matrix-green sheet. The residual structures, which were produced at lower temperature in polymer degradation, were not decomposed completely after CO_2 gas mixing which made nonoxidative decomposition condition.[2]

The decomposition of green sheet pair. The decomposition behaviors of individual matrix were investigated in various gas conditions. In the real fuel cell operation, polymer binders were decomposed in the several green sheet stacks. Thus, it is necessary to compare the thermal decomposition of green sheet alone with that of green sheet pairs in the fuel cell operating condition. In addition, the difference of sintered Ni sheet and Ni-green sheet, which were contacted with matrix-green sheet, was studied. Sintered Ni-matrix green sheet pair was composed of sintered Ni sheet and contacted matrix-green sheet, and Ni-matrix green sheet pair was composed of not sintered Ni-green sheet and contacted matrix-green sheet.

Figure 5 shows decomposition behaviors of Ni-matrix green sheet pair, and sintered Ni-matrix green sheet pair

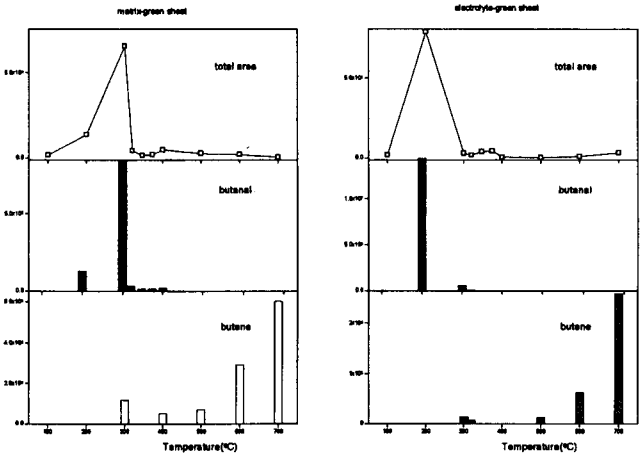

Figure 4. The decomposition behavior of binders in the matrix-green sheet and electrolyte-green sheet when CO_2 mixed with air above 320 °C.

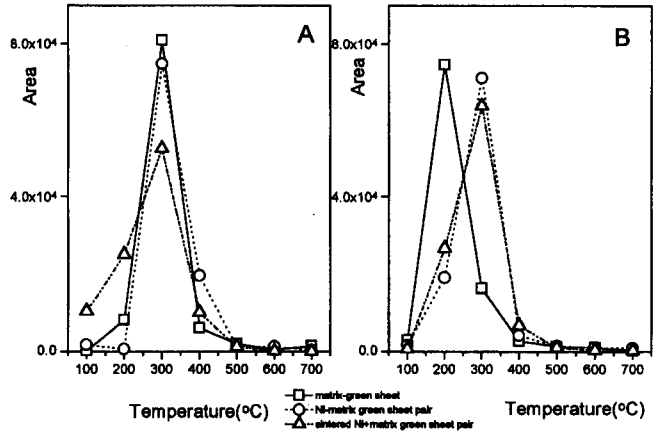

Figure 5. Total GC area changes of Ni-matrix green sheet pair and sintered Ni-matrix green sheet pair. A; air B; air-containing water vapor.

about temperature in two atmospheric conditions; air and air containing water vapor. To see the influence of contacted Ni sheet for decomposition of binders in the matrix-green sheet, the results were compared with that of matrix-green sheet only. The total area changes of produced gases in green sheet pair showed the tendency similar to those in each pair. Sintered Ni-matrix green sheet pair began to decompose at lower temperature than the Ni-matrix green sheet pair.

In air atmospheric condition, the temperatures corresponding to peak maxima of two pairs were nearly same, but the decomposition of matrix-green sheet began at lower temperature than that of other pairs. Sintered Ni-matrix green sheet pair was decomposed at lower temperature than Ni-matrix green sheet pair. The type and decomposition feature of produced gases of two pairs were similar each other.

There was a tendency that the decomposition of binder began to occur at lower temperature when water vapor was added to air.[10] The decomposition of matrix-green sheet was getting faster in air-containing water vapor and both of the two pairs decomposed more significantly at 200 °C, too. The decomposition of sintered Ni-matrix green sheet pair began to occur at somewhat lower temperature than Ni-matrix green sheet pair in air-containing water vapor.

As shown in butanal profiles in Figure 6, the decomposition behavior of the binders in the green sheet pair was very much like the one which was found at the decomposition of binders in the each green sheet, where degradation occurred rapidly around 300 °C in air. The thermal decomposition of sintered Ni-matrix-green sheet pair began at lower temperature than Ni-matrix green sheet pair in pure air, but all of two pairs were decomposed significantly at 200 °C when water vapor was added to the air.

To see the effect of sintering for binder decomposition in the green sheet pair that contains Ni metal, the decomposition of sintered Ni-matrix green sheet pair and Ni-matrix green sheet pair was compared. The butene peak profiles in Figure 7 show termination level of the decomposition reaction for each pair. In contrast to decomposition of individual green sheet, produced butene peak decreased at 700 °C for both green sheet pairs in air. The quantity of butene produced from sintered Ni-matrix green sheet pair was less than that of Ni-matrix green sheet pair under both conditions.

This result means that sintering the electrode is more effective than in-situ burnout for the decomposition of binders as we expected. The binders in the green sheet stack were decomposed slower than single green sheet. The contact surface with air in the green sheet stack was decreased because oxidative gases should pass through the outer sheet to inside. The decomposition of binder in sintered Ni-matrix green sheet pair was more effective than not sintered Ni-matrix green sheet pair because sintered Ni sheet had more suitable porous structure to pass air than Ni-green sheet and residual carbon was effectively eliminated during sintering process. In addition, air-containing water vapor promoted the decomposition of green sheet pair at lower temperature like the decomposition of each green sheet.

Binder burnout in a unit cell. In the binder burnout of a real unit cell, temperature condition and gas atmospheric conditions are somewhat different from that in furnace. Comparing to furnace condition, heating rate (0.2 °C/min-0.4 °C/min) was very slow and sometimes isothermal. Decomposition onset temperature is lowered in slow heating rate because equilibrium can reach more effectively, as shown in the general TG result of neat PVB.[11] The amount of carbonaceous residue formed during binder burnout decrease with increasing temperature and heating rate, but those factors did not affect its chemical reactivity.[9] In the unit cell operation, variables are temperature, heating rate, and gas atmosphere. By decreasing heating rate, the decomposition of binder will proceed better, but the amount of residual carbon will be remained more. Therefore, these two conflicting factors must be controlled properly to completely decompose binders before gas changes.

Anode and cathode were supplied with different gases, but binder burnout process occurred mainly in the electrolyte-matrix stack between anode and cathode. Electrodes were sintered before installation at 850 °C which temperature is higher than unit cell operating temperature. Therefore, most of binder in electrode eliminated by sintering process, and decomposable components were remained in the

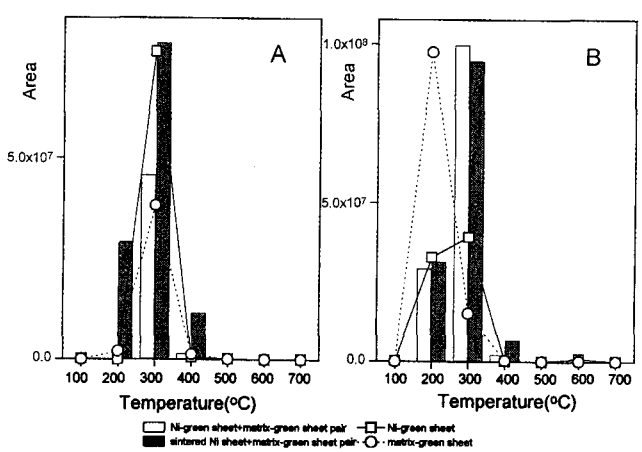

Figure 6. The butanal profiles of Ni-matrix green sheet pair and sintered Ni-matrix green sheet pair. A; air B; air-containing water vapor.

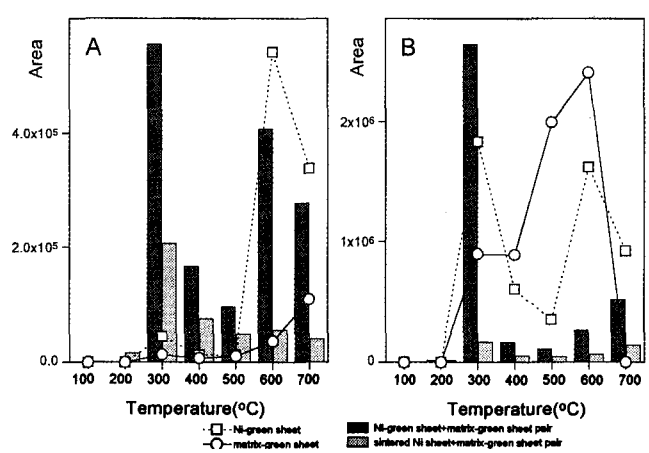

Figure 7. The butene profiles of Ni-matrix green sheet pair and sintered Ni-matrix green sheet pair. A; air B; air-containing water vapor.

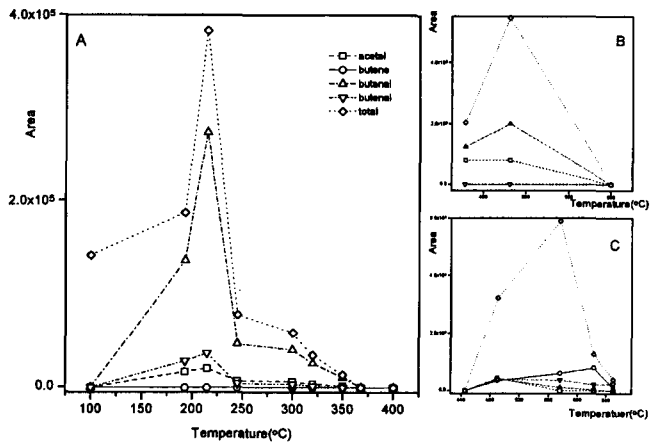

Figure 8. Area *vs.* temperature profiles of major produced gases at the thermal decomposition of a unit cell. Sampling position; A; a gap between two electrodes B; cathode outlet C; anode outlet.

matrix and electrolyte sheet. The decomposition products were analyzed to check the binder burnout in real unit cell based upon results of individual decomposition in each condition.

Figure 8 shows the profiles of major decomposed products in the unit cell operation. The amounts of detected gases in the unit cell were smaller than that in furnace because unit cell was opened and produced gases escaped from its body below electrolyte melting point. Nevertheless, the formation of major decomposed gases including index peaks, butanal and butene were similar with that of the decomposition in furnace. Most of binders were decomposed before the gas changing temperature that was 320 °C, as we expected. The decomposition onset temperature was lowered under sufficient slow initial heating rate and adequate gas conditions.

The amounts of decomposition products were decreased remarkably in a gap between two electrodes above 370 °C when electrolyte-green sheet was almost dispersed to the electrodes and unit cell was wet sealed. Major peaks still remained above 400 °C but the amounts of produced gases were very small in the gas collecting position between two electrodes. Binders had been decomposed effectively before the gases changed to nonoxidative condition below 400 °C.

The butene, index peak was produced only small amount at high temperature. The produced gases in electrode outlet did not disappear even at higher temperature. The total area was higher than the sum of major peaks in Figure 8 B and C because of formation of early-eluting unidentified volatile gases. Butene peak that indicates the terminal state of burnout did not disappear until 620 °C in anode outlet but it was completely disappeared at 650 °C. Butene was not detected in cathode outlet because it was maintained enough oxidative condition. Therefore, we could safely assume that fuel cell began to operate at 650 °C after all binders were eliminated. We set an isothermal period of 9 hrs at 320 °C to completely decompose the binders but that did not make a significant change.

Conclusions

The thermal decomposition of matrix-green sheet and electrolyte-green sheet in CO_2, sintering effect of Ni-green sheet for the decomposition of matrix-green sheet, and binder burnout in unit cell operation were studied. PVB decomposed incompletely in CO_2. Especially, a thermal decomposition of binders in the electrolyte-green sheet were affected by CO_2. Therefore, it is important to decompose binders sufficiently in the oxidative condition before gas changes to CO_2.

Sintered Ni-green sheet was more effective in the decomposition of binders than in-situ binder burnout. Butanal and butene were detected at the decomposition of binders in all green sheets including unit cell contained metal substrates. Butene was not detected in the decomposition of neat PVB at high temperature. Therefore, the decomposition state of binders could be checked indirectly by analyzing the change of two peaks among the decomposition products.

Most of the binders were decomposed in unit cell operation. General features of decomposition were nearly the same as that in furnace. Butanal and butene were also detected and we could check the state of decomposition from the changes of those peaks. Most of the binders were decomposed sufficiently in slow heating rate and adequate gas conditions. Binders had been decomposed effectively before gases were changed to nonoxidative condition. Under that condition, small amounts of butene produced only in the anode outlet at high temperature. Therefore, unit cell could be safely assumed that it began to operate at 650 °C after all binders were eliminated.

Acknowledgment. This study has been carried out with the financial support of KEPRI (Korea Electric Power Research Institute) and Korea Science and Engineering Foundation (96-0502-09-01-3).

References

1. Appleby, A. J.; Foulkes, F. R. *Fuel Cell Handbook*; Van Nostrand Reinhold: New York, U. S. A., 1989; p 539.
2. Shin, W. K.; Sacks, M. D.; Scheifflele, G. W.; Sun, Y. N.; Williams, J. W. *Ceram. Trans.* **1988**, *1*, 549.
3. Bakht, F. *Pakistan J. Sci. Ind. Res.* **1983**, *26*(1), 35.
4. Nair, A.; White, R. L. *J. Apply. Poly. Sci.* **1996**, *60*(11), 1901.
5. Baker, B. S.; Maru, H. C. *Proceedings of the 2nd Symposium on Molten Carbonate Fuel Cell Technolog*; Selman, J. R.; Claar, T. D. Ed.; Electrochem. Soc.: Penington, NJ 1990.
6. Cima, M. J.; Lewis, J. A.; Devoe, A. D. *J. Am. Ceram. Soc.* **1989**, *72*(7), 1192.
7. Lewis, J. A.; Cima, M. J. *J. Am. Ceram. Soc.* **1990**, *73*(9), 2702.
8. Sohn, H. Y.; Wall, D. R. *J. Am. Ceram. Soc.* **1990**, *73*(10), 2953.
9. Masia, S.; Calvert, P. D.; Rhine, W. E.; Bowen, H. K. *J. Mat. Sci.* **1989**, *24*, 1907.
10. Wall, D. R.; Sohn, H. Y. *J. Am. Ceram. Soc.* **1990**, *73*(10), 2944.
11. Seo, J. J.; KuK, S. T.; Kim, K. *J. Power Source* **1997**, *69*, 61.
12. Seo, J. J.; KuK, S. T.; Kim, K. *J. Kor. Chem. Soc.* **1996**, *40*(3), 180.